

ChemComm

Accepted Manuscript



This is an *Accepted Manuscript*, which has been through the Royal Society of Chemistry peer review process and has been accepted for publication.

Accepted Manuscripts are published online shortly after acceptance, before technical editing, formatting and proof reading. Using this free service, authors can make their results available to the community, in citable form, before we publish the edited article. We will replace this *Accepted Manuscript* with the edited and formatted *Advance Article* as soon as it is available.

You can find more information about *Accepted Manuscripts* in the [Information for Authors](#).

Please note that technical editing may introduce minor changes to the text and/or graphics, which may alter content. The journal's standard [Terms & Conditions](#) and the [Ethical guidelines](#) still apply. In no event shall the Royal Society of Chemistry be held responsible for any errors or omissions in this *Accepted Manuscript* or any consequences arising from the use of any information it contains.



Journal Name

COMMUNICATION

Multiple-Color Aggregation-Induced Emission (AIE) Molecules as Chemodosimeters for pH Sensing

Received 00th January 20xx,
Accepted 00th January 20xx

Qi Feng,^a Yuanyuan Li,^b Lili Wang,^a Chen Li,^a Jinmin Wang,^a Yuanyuan Liu,^a Kai Li,^{*a} and Hongwei Hou^{*a}

DOI: 10.1039/x0xx00000x

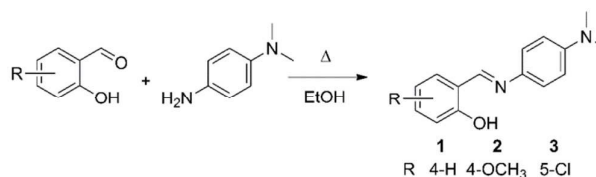
www.rsc.org/

A series of 4-N,N-dimethylaminoaniline salicylaldehyde Schiff-base derivatives (DAS) were facily prepared. They exhibit typical AIE properties with various fluorescence emissions and high fluorescence quantum yields in aggregated state. DAS exhibit unique pH-dependent optical properties, which indicated their potential applications in pH sensing.

pH is one of the key parameters in environmental and biological samples.¹ For measuring pH values, organic fluorescent probes have been widely used due to their structural simplicity, non-destructive emission signals, and capability of real-time detection.² One of the biggest challenge in the wide application of conventional organic fluorophores is from aggregation-caused quenching (ACQ): the fluorogens show good fluorescence in dilute solutions but weak even no fluorescence in concentrated solution or solid state due to the self-quenching effect of adjacent molecules.³ In 2001, a novel luminescence phenomenon of aggregation-induced emission (AIE) was first discovered by Tang and co-workers, which was described from the mechanism of restricted intramolecular rotations (RIR).⁴ In the single molecule state, the conjugate plane such as phenyl rings and heterocyclic rings in AIE molecule undergo dynamic intramolecular rotations, resulting in excited state non-radiative transition and fluorescence quenching. In the aggregated state, the rotations are greatly restricted, which make the radiative transition to be the primary pathway for the excited state electrons back to ground state.⁵ According to the RIR mechanism, a series of AIE molecules have been developed including tetraphenylethene (TPE), hexaphenylsilole (HPS), 1-methyl-pentaphenylsilole (MPPS), 1,1-dimethyl-2,3,4,5-tetraphenylsilole (DMTPS),

distyreneanthracene (DSA), 2,3-dicyano-5,6-diphenylpyrazine, organoboron complexes and salicylaldehyde azine (SAA), and so on, which are widely applied in the development of novel luminogenic materials.⁶ Nevertheless, even though it is quite simple in molecular design, the synthesis of these AIE compounds is often complicated mainly due to the difficulty in forming the C-C single bond linkage of the conjugate planes. Specially, multicolor AIE fluorogens for pH detection is still rare and limited in use, and is in serious need of development in synthesis and application.⁷

In this work, a series of AIE luminogenic compounds based on 4-N,N-dimethylaminoaniline salicylaldehyde (DAS) were developed. AIE luminophor based on salicylaldehyde Schiff-base was first reported by Tong et. al., in which the traditional C-C single bonds are replaced by N-N single bond or C-N single bond thus it significantly simplified the synthesis.⁸ DAS molecules can also be facily prepared. They exhibit typical AIE properties with various fluorescence emissions from green to red and high fluorescence quantum yield in aggregated state. Specially, we discovered for the first time that the DAS compounds exhibit unique pH-dependent optical properties: Different DAS compound shows different titration jump pH, which indicated their potential application prospects in chemodosimeters for pH sensing.



Scheme 1. Synthesis of DAS compounds **1-3**.

As shown in Scheme 1, compounds **1-3** were prepared by one-step synthesis with all inexpensive reagents and favourable yields (85% for **1**, 75% for **2** and 73% for **3**). They were characterized by NMR spectra and ESI-MS spectra. The detailed synthetic procedures and characterization data are given in Supplementary Information. Compound **1-3** are convenience to synthesis with lower cost. Single crystals of **1-3** were grown from methanol/tetrahydrofuran mixtures by slow

^a College of Chemistry and Molecular Engineering, Zhengzhou University, Henan 450001, P. R. China. E-mail: likai@zzu.edu.cn or houhongw@zzu.edu.cn.

^b School of Chemistry and Chemical Engineering, Henan University of Technology, Henan 450001, P. R. China.

Electronic Supplementary Information (ESI) available: Synthesis and characterization, materials, procedures of all experiments; Fluorescence dynamics parameters; and detailed crystal data and structure refinement for **1-3**. CCDC reference numbers 1434488, 1434487 and 1434472. For ESI and crystallographic data in CIF or other electronic format see: 10.1039/x0xx00000x

solvent evaporation and were characterized by X-ray crystallography. All the crystals are stable to moisture, atmosphere and light exposure. They are soluble in common organic solvents such as tetrahydrofuran, dichloromethane, acetonitrile, and so on, but insoluble in water. The crystal structures are shown in Figure S1-S3. For all of these compounds, intramolecular hydrogen bonds in salicylaldehyde moiety could be clearly observed, suggesting there was two conjugated moieties connected by a rotatable single bond in each molecular.^{8a,9} Meanwhile, No face-to-face π - π stacking could be found in the crystals, as deduced from the large intermolecular distances (over 3.8 \AA ¹⁰) in the packing diagram. These structural features indicated that **1-3** had potential of AIE properties by inhibition of free intramolecular rotation in their aggregate state.

The fluorescence characteristics of **1-3** were investigated in ethanol/water (water fraction (f_w) from 0% to 99%, v/v) buffered by 10 mmol/L PBS at pH 7.0. As shown in Figure 1A-1C, the fluorescence emission of **1** was weak in ethanol and increased slowly until f_w reached 70%. Afterwards, the fluorescence emission rose swiftly, which increased by 19-fold from the ethanol solution to 99% aqueous mixture. **2** and **3** behaved similarly (Figure 1D-1I): they exhibited weak fluorescence emission in ethanol solution and in ethanol/water mixtures with f_w lower than 60% and 50%, respectively. When f_w were beyond 60% and 50%, their fluorescence emissions enhanced remarkably, which increased by 32-fold and 14-fold from the ethanol solution to 99% aqueous mixture, respectively. Interestingly, **1-3** exhibited different emissions from green to red: the corresponding maximum emission wavelengths are 542 nm, 513 nm and 580 nm, respectively. These might be due to the electronegative of substituent groups on the salicylaldehyde moiety, which influenced the electronic cloud distribution of the molecule. Compared with some classical AIE molecules, DAS molecules have longer emissions (Table S1).

The fluorescence spectra indicated that **1-3** showed typical AIE characteristics. To further verify that the emission enhancement was from aggregation, the absorption of **1-3** were measured. In ethanol, **1-3** showed absorption peaks at 384, 380, and 394 nm, respectively. However, when they were in a poor solvent of 99% water/EtOH, the fine structures of absorption spectra disappeared and level-off tails in the visible region could be clearly observed (Figure S4), which is believed due to the light scattering of aggregates suspensions.¹¹ Beside absorption spectra and fluorescence spectra, a more direct evidence for the aggregation of **1-3** in poor solvent were obtained from dynamic light scattering (DLS) measurements: no particle could be observed for **1-3** in ethanol, while particles of nanometer or micrometer sizes were detected in aqueous solution (Figure S5-S7).

According to the reports, RIR in the aggregates is identified as a main cause for the AIE effect.^{5,9a,12} This explanation was supported by the emission enhancement of **1-3** in solvents with high viscosity (ethanol/glycerin). As shown in Figure S8-S10, with the increase of glycerin fraction (f_g), the fluorescence emission of **1-3** enhanced gradually. Meanwhile, no level-off

tail could be observed in their absorption spectra which suggested there was no aggregate of **1-3** in glycerine (Figure S11-S13).

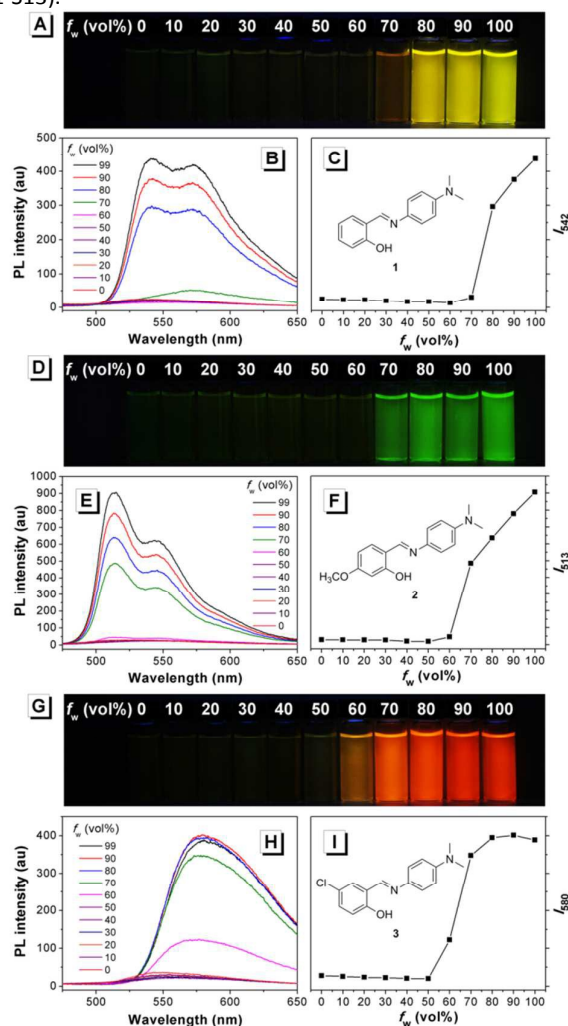


Figure 1. (A, D, G) Fluorescence photographs and (B, E, H) fluorescence emission spectra of **1-3** in water/EtOH mixtures with different f_w . (C, F, I) Fluorescence emission peak intensities of **1-3** as function of f_w . Conditions: The concentrations of **1-3** are $50 \mu\text{mol/L}$. The excitation wavelengths of **1-3** are 333, 338 and 356 nm, respectively. The photographs are taken under an irradiation of 365 nm UV light.

Fluorescence dynamics provides plentiful information to understand the photophysical process and emission mechanism of AIE molecules. The lifetime (τ) of **1-3** were measured to be 2.54, 0.93 and 2.27 ns, respectively. According to the definition of $\tau = 1/(k_r + k_{nr})$ and $\phi = k_r/(k_r + k_{nr})$, the excited-state decay rate constant can be estimated as $k_r = \phi/\tau$ and $k_{nr} = (1 - \phi)/\tau$ (ϕ is the fluorescence quantum yield, k_r and k_{nr} are the radiative decay rate constant and non-radiative decay rate constant, respectively).¹³ The calculated k_r and k_{nr} values of **1-3** are listed in Table S2. Remarkably, the k_r and k_{nr} values of **1-3** are close to each other, which indicate their analogous radiative and non-radiative decay process. This

result is consistent with the similar molecule structure and spatial configuration of **1-3**. The fluorescence quantum yields of **1-3** are 14.9%, 7.4% and 8.0%, which are comparable to the reported AIE molecules based on salicylaldehyde Schiff-base.^{8, 14} The various emission wavelengths of **1-3** may be due to the electronic structure difference of the molecules. In order to gain insight into the electronic structures of **1-3**, theoretical calculations were performed with Gaussian 09 program. The geometries were optimized with B3LYP hybrid density function and the basis set used was 6-31G*. The geometries of the optimized molecular structures are very similar to their conformations in the crystalline state, where the dihedral angles between salicylaldehyde plane and phenylamine plane are less than 3.29 degrees (All the atoms except hydrogen are nearly in the same plane). Frontier molecular orbitals and energy levels of the HOMOs and the LUMOs of **1-3** are shown in Figure 2. The distribution of HOMO and LUMO for all of **1-3** are very similar, which induce comparable AIE properties. Energy gap between HOMO and LUMO (EHL) is correlated with the wavelength of fluorescence emission: Small EHL enables the electron transit easily result in a red-shifted fluorescence emission. The calculated results of EHL are well consistent with the fluorescence emission obtained by experiments: The maximum emission wavelengths of **1-3** are 542 nm, 513 nm and 580 nm, while the corresponding EHL are 5.73 eV, 5.80 eV and 5.60 eV, respectively.

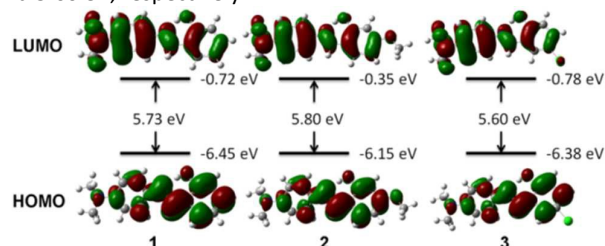


Figure 2. Frontier molecular orbital amplitude plots and energy levels of the HOMOs and the LUMOs of **1-3**. Value of contour envelopes is 0.02 au.

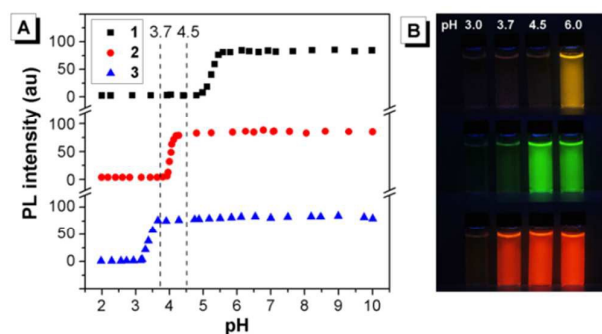


Figure 3. (A) Fluorescence emission peak intensities of **1-3** as function of pH value. (B) Fluorescence photographs of **1-3** in 99% water/EtOH (v/v) at different pH value. Conditions: The concentrations of **1-3** are 50 $\mu\text{mol/L}$. The excitation/emission wavelengths of **1-3** are 333/542, 338/513, 356/580 nm, respectively. The photographs are taken under an irradiation of 365 nm UV light.

The effect of pH on fluorescence was investigated for **1-3** in aqueous solution ($f_w = 99\%$) buffered by PBS at pH 2.0-10.0.

Interestingly, they exhibited strong fluorescence emission in alkaline condition and different pH-dependent fluorescence response in acid condition. As shown in Figure 3A, **1-3** showed titration jump at the pH around 5.3, 4.1 and 3.5, respectively. Figure 3B gave a fluorescence photo at different pH value. Notably, the addition of excess base to acid solution couldn't recover the fluorescence of **1-3**, but new fluorescence peaks around 500 nm could be observed, which were similar to that of their corresponding salicylaldehyde derivatives (**4-6**) in same conditions (Figure S14-S16). These results suggested **1-3** undergo irreversible reactions with acid. Compared with previous reported molecules,^{7a} DAS molecules as chemodosimeters for pH sensing have the advantages of multiple-color and different pH-dependent fluorescence response. The reversible switching of fluorescence emission upon pH change was not achieved, which is a limitation for DAS and most of the chemodosimeters.¹⁵

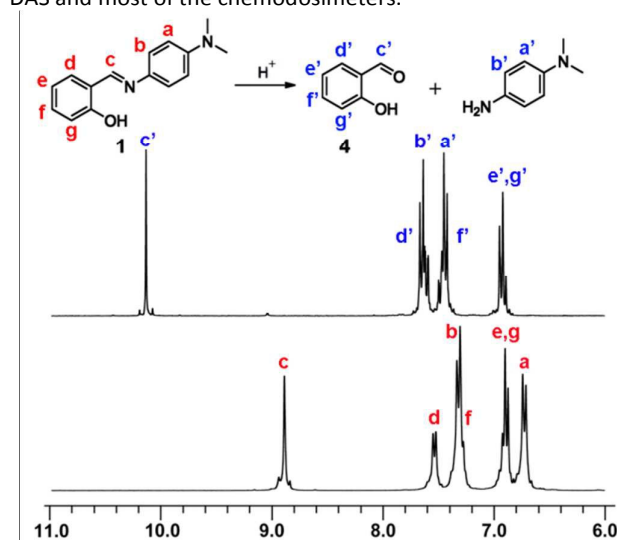


Figure 4. ¹H-NMR spectra of **1** in 500 μL DMSO- d_6 before and after the addition of 20 μL TFA/ D_2O (1:9 v/v).

To understand the pH response of **1-3**, a possible mechanism was proposed (Figure 4 and Figure S17-S18): the electron donor group of N,N-dimethylamino in phenylamine moiety increases the electron density of C=N bond, thus the protons in acid solutions could attack the double bonds easily by electrophilic substitution, resulting in a 4-N,N-dimethylaminoaniline and corresponding salicylaldehyde derivatives. To confirm this assumption, a series of experiments were carried out. In the absorption spectra of **1-3**, the level-off tails in the visible region disappeared when pH changes from 7.0 to 3.0, which suggested the aggregates were interfered and destroyed in acid (Figure S19-S21). These results were consistent with DLS tests: no particle could be observed for **1-3** in pH 3.0 solution. More direct evidences for the hydrolysis reaction of **1-3** were observed from the ¹H-NMR spectra. Figure 4 shows the ¹H-NMR spectra (aromatic proton peaks) of **1** in neutral and acidic conditions. In DMSO- d_6 / D_2O mixtures, **1** exists in its original form and its proton resonance peaks are well assigned with red letters. After addition of

trifluoroacetic acid (TFA) into the mixture, most of the protons signals are shifted to the low field as indicated with blue letters. In particular, the proton c assigned to Schiff-base protons has a large chemical shift change about 1.2 ppm after the pH change. This unusual change clearly showed the formation of formyl group: oxygen is more electronegative than nitrogen, thus proton c' has a lower chemical shift than proton c. As shown in Figure S17-S18, analogous results were obtained for **2** and **3**. In addition, results from ESI-MS spectra were consistent with that of the ¹H-NMR spectra. In neutral condition, only the molecular ion peaks of **1-3** were obtained. After treatment with acid, different molecular ion peaks of salicylaldehyde derivatives and 4-N,N-dimethylaminoaniline could be clearly observed (Figure S22-S24).

Generally, the C=N bond in Schiff-base is stable in a wide range of pH value in room temperature,^{8a, 16} and compounds **1-3** were stable in alkaline or neutral condition as well (Figure S25). However, **1-3** exhibited different stability in acidic condition, which is due to the negative inductive effect of substituent groups in salicylaldehyde moiety. Normally, the hydrolysis of Schiff-base in acid solution is ascribed to an electrophilic addition reaction. The electron density of C=N bond dominates the stability of Schiff-base. Chlorine in meta-position has high electronegativity, which reduces the electron density of C=N bond in Schiff-base. Thus, higher hydrogen ion concentration was needed to hydrolyze the C=N bond in **3**. The methoxyl in para-position also exhibited inductive effect. Compared with chlorine, the methoxyl has weaker negative inductive effect and longer distance from the C=N double bond. Thus, the titration jump of **2** occurred in a higher pH than that of **3**. For compound **1**, there is no negative inductive effect substituent groups in salicylaldehyde moiety, so the C=N double bond in **1** has the lowest stability.

In summary, a series of luminogenic compounds based on 4-N,N-dimethylaminoaniline salicylaldehyde (DAS) were developed. They exhibit typical AIE properties with various fluorescence emissions from green to red and high fluorescence quantum yields in aggregated state. DAS can be facilely prepared by one-step synthesis with all inexpensive reagents and favourable yields. DAS compounds exhibit unique pH-dependent optical properties: Luminous DAS compound can be hydrolyzed in acid conditions, result in a nonluminous mixture of 4-N,N-dimethylaminoaniline and corresponding salicylaldehyde derivatives. The different substituent groups in salicylaldehyde moiety produce the difference of titration jump pH, which indicate their potential application prospects in pH sensing. This work offers a new direction for developing pH chemodosimeter based on AIE luminophore. Efforts on the development of more DAS-based multifunctional AIE system are in progress in our laboratories.

This work was supported by the National Natural Science Foundation of China (No.21501150, 51502079, 21371155), Research Found for the Doctoral Program of Higher Education of China (20124101110002). We are grateful for the helpful advices in our experiments from Benzhong Tang's lab of HKUST.

Notes and references

1. J. R. Casey and S. J. Grinstein, *Nat. Rev. Mol. Cell Biol.*, 2010, **11**, 50-61.
2. a) S. Chen, J. Liu, Y. Liu, H. Su, Y. Hong, C. K. Jim, R. T. Kwok, N. Zhao, W. Qin and J. W. Lam, *Chem. Sci.*, 2012, **3**, 1804-1809; b) Z. Yang, W. Qin, J. W. Lam, S. Chen, H. H. Sung, I. D. Williams and B. Z. Tang, *Chem. Sci.*, 2013, **4**, 3725-3730; c) S. Chen, Y. Hong, Y. Liu, J. Liu, C. W. Leung, M. Li, R. T. Kwok, E. Zhao, J. W. Lam and Y. Yu, *J. Am. Chem. Soc.*, 2013, **135**, 4926-4929.
3. J. B. Birks, *Photophysics of Aromatic Molecules*, Wiley, New York, 1970.
4. J. Luo, Z. Xie, J. W. Lam, L. Cheng, H. Chen, C. Qiu, H. S. Kwok, X. Zhan, Y. Liu and D. Zhu, *Chem. Commun.*, 2001, 1740-1741.
5. J. Chen, C. C. Law, J. W. Lam, Y. Dong, S. M. Lo, I. D. Williams, D. Zhu and B. Z. Tang, *Chem. Mater.*, 2003, **15**, 1535-1546.
6. a) Y. Hong, J. W. Lam and B. Z. Tang, *Chem. Commun.*, 2009, 4332-4353; b) Y. Hong, J. W. Lam and B. Z. Tang, *Chem. Soc. Rev.*, 2011, **40**, 5361-5388; c) D. Dan, L. Kai, L. Bin and B. Z. Tang, *Acc. Chem. Res.*, 2013, **46**, 2441-2453; d) Z. Zhao, B. He and B. Z. Tang, *Chem. Sci.*, 2015, **6**, 5347-5365; e) H. Rongrong, N. L. C. Leung and T. Ben Zhong, *Chem. Soc. Rev.*, 2014, **43**, 4494-4562.
7. a) J. Tong, Y. Wang, J. Mei, J. Wang, A. Qin, J. Z. Sun and B. Z. Tang, *Chem. - Eur. J.*, 2014, **20**, 4661-4670; b) D. Wu, L. Shao, Y. Li, Q. Hu, F. Huang, G. Yu and G. Tang, *Chem. Commun.*, 2015, DOI: 10.1039/C5CC08429F; c) Z. Zhou, F. Gu, L. Peng, Y. Hu and Q. Wang, *Chem. Commun.*, 2015, **51**, 12060-12063.
8. a) W. Tang, Y. Xiang and A. Tong, *J. Org. Chem.*, 2009, **74**, 2163-2166; b) P. Song, X. Chen, Y. Xiang, L. Huang, Z. Zhou, R. Wei and A. Tong, *J. Mater. Chem.*, 2011, **21**, 13470-13475.
9. a) M. Ju, H. Yuning, J. W. Y. Lam, Q. Anjun, T. Youhong and T. Ben Zhong, *Adv. Mater.*, 2014, **26**, 5429-5479; b) R. Zhang, M. Gao, S. Bai and B. Liu, *J. Mater. Chem. B*, 2015, **3**, 1590-1596.
10. C. Janiak, *J. Chem. Soc., Dalton Trans.*, 2000, 3885-3896.
11. H. Auweter, H. Haberkorn, W. Heckmann, D. Horn, E. Lüddecke, J. Rieger and H. Weiss, *Angew. Chem. Int. Ed.*, 1999, **38**, 2188-2191.
12. a) A. Qin, J. W. Y. Lam, F. Mahtab, C. K. W. Jim, L. Tang, J. Sun, H. H. Y. Sung, I. D. Williams and B. Z. Tang, *Appl. Phys. Lett.*, 2009, **94**, 253308; b) J. Shi, N. Chang, C. Li, J. Mei, C. Deng, X. Luo, Z. Liu, Z. Bo, Y. Q. Dong and B. Z. Tang, *Chem. Commun.*, 2012, **48**, 10675-10677.
13. Z. F. Chang, L. M. Jing, C. Wei, Y. P. Dong, Y. C. Ye, Y. S. Zhao and J. L. Wang, *Chem. - Eur. J.*, 2015, **21**, 8504-8510.
14. Y. Mingdi, X. Dongling, X. Wengang, W. Lianke, Z. Jun, H. Jing, Z. Jingyan, Z. Hongping, W. Jieying and T. Yupeng, *J. Org. Chem.*, 2013, **78**, 10344-10359.
15. Y. Yang, Q. Zhao, W. Feng, F. Li, *Chem. Rev.*, 2013, **113**, 192-270.
16. a) K. Li and A. Tong, *Sens. Actuators, B*, 2013, **184**, 248-253; b) K. Li, X. Wang and A. Tong, *Anal. Chim. Acta*, 2013, **776**, 69-73.